Journal of Design Against Fatigue
https://minerva-aset.com/JDAF

MINERVA ASET ISSN 2976-940X

Experimental research on mechanical and material properties of Inconel 600: Application in elevated temperature environment

A. Moradi [a], S. Ghorbani [b], M. Chizari [a,*]

a School of Physics, Engineering & Computer Science, University of Hertfordshire, Hatfield AL10 9AB, UK.
b Department of Mechanical Engineering Technologies, Academy of Engineering, RUDN University, 6 Miklukho-Maklaya St, Moscow, 117198, Russian Federation.

P A P E R I N F O

Paper history:
Received 9 February 2024
Received in revised form 28 February 2024
Accepted 29 February 2024

Keywords:
Inconel 600
Fatigue
Creep
Mechanical properties
High temperature

A B S T R A C T

Abstarct Due to high strength and toughness, high oxidation resistance, and high ductility, the Inconel 600 alloy is an ideal choice for the components used in combined heat and power turbines. Therefore, in this paper, the authors conducted experimental tests in order to better understand the mechanical behavior of superalloys Inconel 600. The experiments included tensile, fatigue, and creep tests. By conducting the tensile test, the yield strength, ultimate tensile strength, elongation, and modulus of elasticity were captured. By illustrating the engineering and true stress-strain curves the Ramberg-Osgood relation were extracted. As a result of fatigue test, the relationship between strain amplitude and the number of cycles to failure for specimens were obtained. The creep tests were conducted at a constant temperature of 650°C. The strain-time data were collected, and the resulting creep strain-time curve were plotted for smooth samples under their respective stress conditions.

doi: *https://doi.org/10.62676/jdaf.2024.2.1.30*

1. INTRODUCTION

Inconel 600 is an austenitic and stable solid-solution nickel-chromium based superalloys. It is non-magnetic, has excellent mechanical properties, and provides the desired combination of high strength and good weldability over a wide temperature range [1-2]. Inconel 600 has excellent resistance to oxidation at high temperatures. It can withstand temperatures up to 2200°F (1204°C) before corroding. The removed grain boundaries of supperalloy 600 results in the incipient melting temperature. In addition, it can be heat treated at a higher temperature [3]. These properties make it suitable for use in extreme environments in aerospace components such as blades, shafts, aircraft engines, hot water pipes, and the steam generators in nuclear power plants in which it is required to control the microstructure of the hot-worked component [4-6].

Inconel 600 has excellent corrosion resistance when exposed to seawater, steam, or other substances containing chlorides or sulfates. This property makes it ideal for use in marine environments, where it may come into contact with salt water throughout its life [7]. In addition, the high nickel content of Inconel 600 gives it high resistance to chloride ion stress corrosion cracking [8]. The high-temperature mechanical properties of Inconel 600 are affected by many factors such as microstructural changes and flow characteristic [9] in particular strain, strain rate, and temperature [10]. For instance, turbine blades are subjected to high stresses,

*Corresponding Author Email: m.chizari@herts.ac.uk (Mahmoud Chizari)

Cite this article as: A. Moradi, S. Ghorbani, and M. Chizari. Experimental research on mechanical and material properties of Inconel 600: Application in elevated temperature environment, ***Journal of Design Against Fatigue,*** Vol. 2, No. 01, (2024), 21-27, *https://doi.org/10.62676/jdaf.2024.2.1.30*

temperatures, and vibration environment leading to fatigue failures, fracture, blade failures, yielding or creep failures, which can destroy the turbine blades and the engine [11]. Therefore, understanding the mechanical behavior of superalloys is a key factor to guarantee the workability and controlling the microstructural evolution at high temperatures. Li and Lin [12] investigated the mechanical property and Vickers hardness of Inconel 600 due to strengthening with electric current stressing. The strengthening mechanism was investigated in terms of grain size, grain orientation, phase transformation, dislocation, and precipitation. Ki et al. [13] indicated that increase in static load under critical static load refines the grain size leading to an improved grain boundary diffusion and strength passive film. It also induces the compressive residual stress by enhancing the surface diffusion and passivation of Inconel 600. Kuzmanov et al. [14] conducted tensile test of Inconel 600 wire at room and high temperatures (700 ºC, 800 ºC, and 900 ºC). It was observed a brittle behaviour of Inconel 600 at room temperature and ductile behavoiur of the material at high temperature. In addition, at high temperature the stress properties decrease. Tensile residual stresses make the material weaker and shortens the life cycle of fatigue leading to corrosion cracking, distortion, stress fatigue cracking, and premature component failures [15-16]. Gajalappa et al. [5] applied thermo-mechanical deformation technique to analyze the flow behaviour of Inconel 600 in the temperature range of 950 ºC to 1100 ºC and strain rate range of 10^{-3} to 1 s^{-1}. At higher strain rate of the true stress-strain curve showed softening and steady state behaviour. Whereas, at lower strain rate the curve showed strain hardening. Horng et al. [6] carried out hot tensile tests of Inconel 600 in the temperature ranges from 850 to 1150 °C and strain rate ranges from 0.001 to 1 s^{-1} and analyzed the softening mechanism of dynamic recrystallization. It was concluded that increase in strain rate increases the dislocation generation, leading to a more significant hardening effect and a higher flow stress. Horng et al. [9] also showed that softening mechanisms of Inconel 600 is dependent on grain growth and dynamic recrystallization. Kassim et al. [8] evaluated the fatigue crack growth rate of Inconel 600 in air and at room temperature under constant amplitude loading using compact tension specimens. Microstructure and mechanical behaviour of specimens indicated a transgranular and ductile fracture, with a mechanism of void nucleation, growth, and coalescence. Kwon et al. [4] studied the fretting fatigue strength of the Inconel 600 in room temperature and 320 ◦C. They found out that fretting condition caused about 70% of fatigue strength reduction in both temperatures at 10^7 cycles. Waldemar et al. [17] investigated the effect of grain size on the mechanical properties of Inconel 600. The authors claimed that grain size refinement achieved by sever plastic deformation technique leads to a higher strength of Inconel 600 while maintaining enough ductility. Yi and Was [18] discussed the creep mechanism of Alloy 600 MA in terms of stress and temperature from constant load, step-load, and step-temperature tests. They determined the apparent activation energy area as well as the validity of the power law form. It was shown that the internal stress strongly depends on applied stress. Heriberto et al. [1] investigated the creep behaviour of Inconel 625/Inconel 600 welded joints. It was observed that the fracture occurred in Inconel 600 is mainly related to the smaller grain size and the presence of a high fraction of Cr-rich carbides along the grain boundaries.

This paper is focusing on the durability and material characterization of Inconel 600 under cyclic loading and creep condition. For this purpose, first the tensile test was conducted to determine important design mechanical properties including ultimate tensile strength, Young's modulus, and yield strength. The well-known Ramberg–Osgood equation was applied to determine the material behavior. Fatigue test and creep test were carried out. The microstructure analysis of Inconel 600 was also performed using an optical microscope.

2. EXPERIMENTAL PROCEDURE

2.1. Material

The material used in this study was Inconel 600 alloy, which its chemical composition has been summarized in Table 1.

TABLE 1. Chemical composition of Inconel 600 [19]

Comp (%)	Ni	Cr	Fe	C	Mn	S	Si	Cu
Inconel 600	73.63	15.68	8.79	0.054	0.33	0.006	0.24	0.028

Inconel 600 alloy is known for its high strength and toughness, high oxidation resistance, and high ductility [20]. These characteristics make it an ideal choice for the components used in CHP (combined heat and power) turbines in which resistivity against high temperatures and cyclic loadings are essential. Hence, essential mechanical tests have been carried out and material properties have been extracted. The experimental tests, covered in this study are as follows:

1. Tensile tests for Inconel 600
2. Fatigue tests for Inconel 600
3. Creep tests at different loadings under a constant temperature.

2.2. Sample Preparation

In this study, samples for both tensile and fatigue tests were meticulously prepared following the guidelines provided by the ASTM-E8-04 [21] and ASTM E466 [22]. To this end, samples were obtained from Inconel 600 sheets with a uniform thickness of 3 mm. The choice of sheet material ensured homogeneity and minimized variations in mechanical properties throughout the samples. The use of standardized sample dimensions and geometries, as per the designated ASTM E8-04 standard, allowed for direct comparison with existing data and ensured the reproducibility of the results.

2.3. Quasi-Static Tensile Tests

Quasi-static tensile tests were conducted on Inconel 600 samples to characterize its response to static loading conditions. During the tests, the samples were subjected to uniaxial loading at a constant and controlled speed of 1 mm/min. This loading rate allows for the accurate measurement of material deformation and stress-strain behavior, capturing critical mechanical properties such as yield strength, ultimate tensile strength, elngation, and modulus of elasticity.
Engineering and true stress-strain curves are illustrated in Figure 1. The mechanical properties of the Inconel 600 alloy are presented in Table 2.

TABLE 2. Mechanical properties of Inconel 600

	UTS (MPa)	Yield Strength (MPa)	Elongation (%)
Inconel 600	671	345	50.8

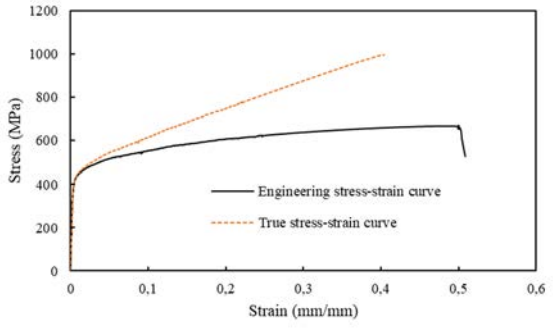

Figure 1. Engineering and true stress-strain curves for Inconel 600

By plotting true stress versus true plastic strain, one can extract the Ramberg-Osgood constants. The Ramberg-Osgood equation is a widely used mathematical model in engineering mechanics to describe the stress-strain relationship in materials beyond their elastic limits (see Figure 2).

The Ramberg-Osgood relation is presented in one of the following forms [23-24]:

$$\varepsilon = \frac{\sigma}{E} + \left(\frac{\sigma}{H'}\right)^{1/n'} \quad (1)$$

$$\sigma = H'(\varepsilon_p)^{n'} \quad (2)$$

where H' and n' are Ramberg-Osgood constants. The Ramberg-Osgood equation is valuable for predicting the non-linear deformation of materials under various loading conditions, making it essential in structural analysis and design. The Ramberg-Osgood constants are summarized in Table 3.

TABLE 3. Ramberg-Osgood constants of Inconel 600

	H' (MPa)	n'	R^2
Inconel 600	771	-0.113	0.98

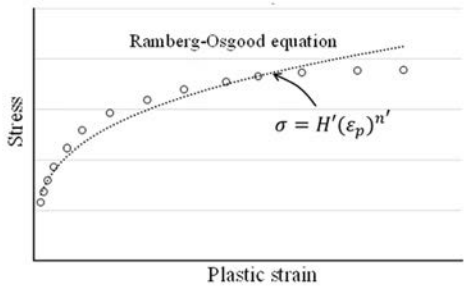

Figure 2. A typical Ramberg-Osgood relation, showing the power-law relationship between stress and plastic strain components

True stress versus true plastic strain for Inconel 600 is shown in Figure 3. Knowing the Ramberg-Osgood parameters are very important to evaluate fatigue life of notched components with different geometries using strain-based approaches. These parameters, along with the Neuber formula (Equation 3) [25] are used to obtain the essential parameters, including strain amplitudes and mean stresses to be used in any strain-based fatigue life prediction models such as SWT criterion.

$$\sigma_{max}\varepsilon_{max} = \frac{(K_t S_{max})^2}{E} \quad (3)$$

In this equation, σ_{max} and ε_{max} are maximum stress and strain at the notch root of a notched component, S_{max} is the maximum remote stress, K_t is the elastic stress concentration factor, and E is Young's modulus.

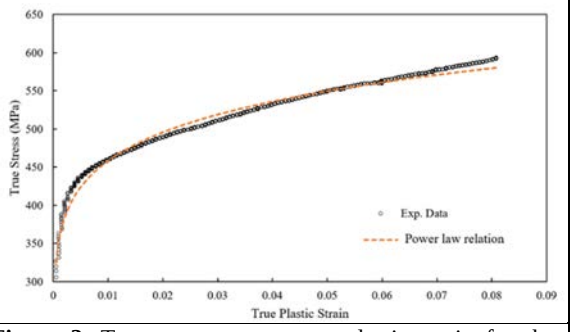

Figure 3. True stress versus true plastic strain for the Inconel 600

3. RESULTS AND DISCUSSION

3.1. Microstructures

A detailed microstructural analysis was conducted using an optical microscope to investigate the grain size and other microstructural features.
Etching was then performed to reveal the microstructure effectively. The microstructural images obtained from the optical microscope, presented in Figure 4.

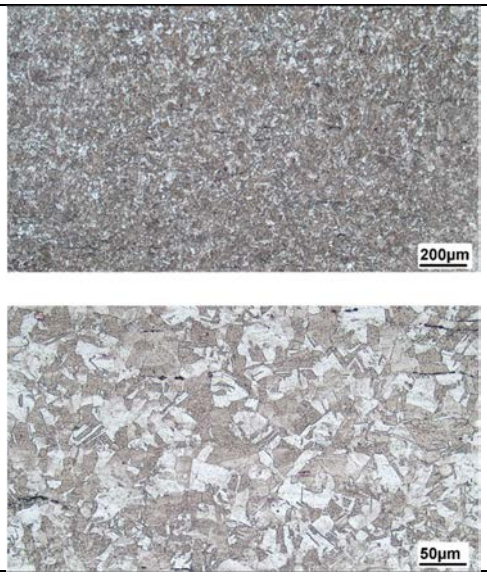

Figure 4. Microstructure images of Inconel 600 with different magnifications

3.2. Fatigue Testing

Fatigue tests on smooth samples were performed using a state-of-the-art Zwick/Roell servo-hydraulic fatigue testing machine with a load ratio R=0 and a testing frequency of 10 Hz, according to ASTM E466 standard [22]. The fatigue behavior of Inconel 600 was thoroughly examined to assess their resistance to cyclic loading.

Figure 5 presents the comprehensive fatigue test data for Inconel 600, and each point represents the average results in three repetitions of the test.

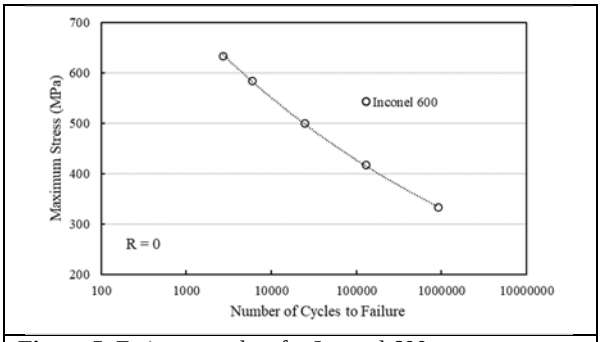

Figure 5. Fatigue test data for Inconel 600

Figure 6 illustrates the relationship between strain amplitude and the number of cycles to failure for specimens. To facilitate accurate fatigue life predictions, the study summarizes the essential strain-based fatigue parameters in Table 4. These parameters are crucial for evaluating the materials' fatigue performance and making reliable assessments of their durability under cyclic loading. To obtain strain-based fatigue parameters, first, the data at the equivalent completely reversed stress condition (R=-1) was obtained using the SWT parameter as follows [26]:

$$\sigma_{ar} = \sqrt{\sigma_{max}\sigma_a} \quad (4)$$

In this equation, σ_{ar} is the equivalent completely reversed stress amplitude, σ_a is the stress amplitude at R=0, and σ_{max} is the maximum stress.

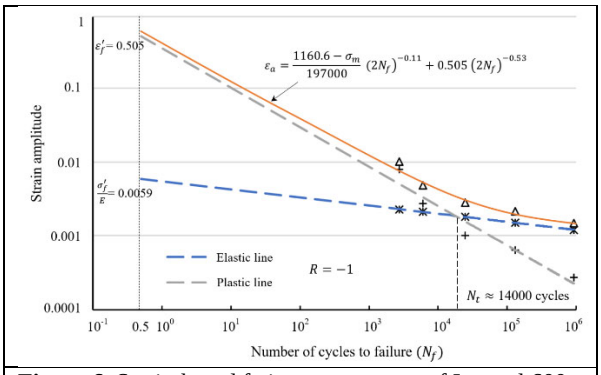

Figure 6. Strain-based fatigue parameters of Inconel 600

TABLE 3. Strain-based fatigue parameters of Inconel 600

Material	σ'_f	b	ε'_f	c
Inconel 600	1160.6	-0.11	0.505	-0.53

3.3. Creep Test

Before conducting the creep tests, the test sample configuration and test setup apparatus were carefully prepared to ensure accurate and reliable results. Figure

7 provides a visual representation of the test sample used in the experiment. In addition, Figure 8 illustrates the test setup apparatus used for the creep testing. The apparatus was designed to control and maintain a constant temperature of 650℃ throughout the testing process. For the smooth sample, stress level of 400 MPa was utilized. This stress level was chosen based on the material properties and the intended application of the samples.

Figure 7. Creep test sample

Figure 8. Test setup apparatus used for the creep testing

During the testing, the creep strain values were continuously monitored at regular intervals over a predetermined time duration. The strain-time data were collected, and the resulting creep strain-time curve was plotted for smooth samples under their respective stress conditions. Figure 9 depicts the creep strain-time response for the smooth sample subjected to a stress of 400 MPa and a temperature of 650℃.

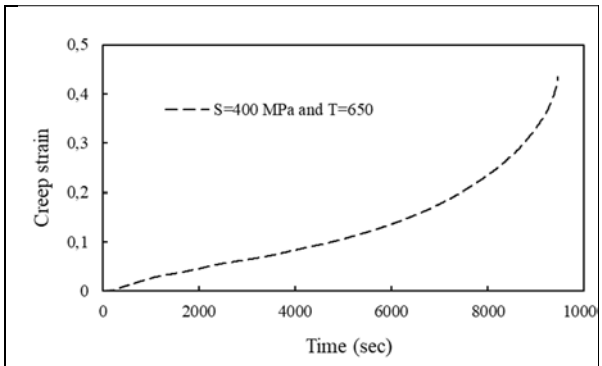

Figure 9. Creep strain versus time for smooth sample at S=400 MPa and T=650℃

As seen in Figure 9, samples failed under creep environment at 650℃, very quickly, indicating that Inconel 600 alloy is not suitable for the applications where creep may occur at high temperatures even at low load levels. However, it has been shown through research studies that, it can tolerate creep loading at lower temperatures like 300-400℃ [27].

4. CONCLUSION

In this paper, the tensile tests, fatigue, and creep tests were conducted to understand the mechanical behavior of Inconel 600. A typical Ramberg-Osgood relation was extracted, which shows the power-law relationship between stress and plastic strain components. Experimental results showed that at temperature 650℃ samples failed. This means that Inconel 600 alloy is not recomended to be applied where creep may occur at high temperatures even at low load levels.

CONFLICTS OF INTEREST

The authors declare that they have no known competing financial interests or personal relationships that could have appeared to influence the work reported in this paper.

REFERENCES

1. H.G. Becerra, M.R.B. Alvarez, V.H.L Morelos, A. Ruiz. Creep behavior and microstructural characterization of Inconel-625/Inconel-600 welded joint. MRS Adv. 8, (2023) 1217–1223, https://doi.org/10.1557/s43580-023-00662-7.
2. A. Baig, S.H.I. Jaffery, M.A. Khan, M. Alruqi, Statistical analysis of surface roughness, burr formation and tool wear in high speed micro milling of Inconel 600 alloy under cryogenic, wet and dry conditions. Micromachines 14(1) 2023, 13. https://doi.org/10.3390/mi14010013.

3. A. Nanaware, S. Pawar, M. Ramachandran. Mechanical characterization of nickel alloys on turbine blades. REST J.E.M.M., 1(1) (2015), 15–19.
4. J.D. Kwon, D.K. Park, S.W. Woo, D.H. Yoon, I. Chung. A study on fretting fatigue life for the Inconel alloy 600 at high temperature. Nucl. Eng. Des. 240 (2010) 2521–2527. https://doi.org/10.1016/j.nucengdes.2010.05.013.
5. Y. Gajalappa, A. Krishnaiah, K.B. Kumar, Eswaranna, K.K. Saxena, P. Goyal. Flow behaviour kinetics of Inconel 600 superalloy under hot deformation using gleeble 3800. Mater. Today: Proc. 45 (2021) 5320–5322. https://doi.org/10.1016/j.matpr.2021.01.909.
6. H.Y. Wu, P.H. Sun, F.J. Zhu, S.C. Wang, W.R. Wang, C.C. Wang, C.H. Chiu. Tensile flow behavior in Inconel 600 alloy sheet at elevated temperatures. Procedia Eng. 36 (2012) 114–120. https://doi.org/10.1016/j.proeng.2012.03.018.
7. T. Xu, S. Wang, X. Tang, Y. Li, J. Yang, J. Li, Y. Zhang. Corrosion mechanism of Inconel 600 in oxidizing supercritical aqueous systems containing multiple salts. Eng. Chem. Res. 58(51) (2019) 23046–23056. https://doi.org/10.1021/acs.iecr.9b04527.
8. K.S. Al-Rubaie, L.B. Godefroid, J.A.M. Lopes. Statistical modeling of fatigue crack growth rate in Inconel alloy 600. Int. J. Fatigue 29 (2007) 931–940. https://doi.org/10.1016/j.ijfatigue.2006.07.013.
9. H.Y. Wu, F.J. Zhu, S.C. Wang, W.R. Wang, C.C. Wang, C.H. Chiu. Hot deformation characteristics and strain-dependent constitutive analysis of Inconel 600 superalloy. J. Mater. Sci. 47 (2012) 3971–3981. https://doi.org/10.1007/s10853-012-6250-4.
10. M.A. Khafri, N. Golarzi. Forming behavior and workability of Hastelloy X superalloy during hot deformation. Mater. Sci. Eng. A 486 (2008) 641–647. https://dx.doi.org/10.1016/j.msea.2007.11.059.
11. A.T.W.K. Fahmi, K.R. Kashyzadeh, S. Ghorbani. A comprehensive review on mechanical failures cause vibration in the gas turbine of combined cycle power plants. Engineering Failure Analysis 134 (2022) 106094. https://doi.org/10.1016/j.engfailanal.2022.106094.
12. W.J. Li, K.L. Lin. Strengthening of Inconel 600 alloy with electric current stressing. MTLA 27 (2023) 101666. https://doi.org/10.1016/j.mtla.2022.101666.
13. K.T. Kim, Y.S. Kim. The effect of the static load in the UNSM process on the corrosion properties of alloy 600. Materials 12 (2019) 3165. https://doi.org/10.3390/ma12193165.
14. N. Kuzmanov, B. Borisov, I. Muhtarov. Tensile testing of Inconel 600 wire at high temperatures. IOP Conf. Ser.: Mater. Sci. Eng. 878 (2020) 012057. https://doi.org/10.1088/1757-899X/878/1/012057.
15. P.V.C.S. Rao, A. Manoj, B.R. Swathi. Residual stress measurement of Inconel 600 on different welding techniques by using conventional and XRD methods. Mater. Today: Proc. 41 (2021) 1160–1163. https://doi.org/10.1016/j.matpr.2020.09.403.
16. K. Reza Kashyzadeh, G.H. Farrahi, A. Ahmadi, M. Minaei, M. Ostad Rahimi, S. Barforoushan. Fatigue life analysis in the residual stress field due to resistance spot welding process considering different sheet thicknesses and dissimilar electrode geometries. Proceedings of the Institution of Mechanical Engineers, Part L: Journal of Materials: Design and Applications. 237(1) (2023) 33-51. https://doi.org/10.1177/14644207221101069.
17. W.A. Monteiro, S.L.V. Silva, L.V. Silva, A.H.P. Andrade, L.C.E. Silva. Characterization of nickel alloy 600 with ultra-fine structure processed by severe plastic deformation technique (SPD). J. Mater. Sci. Chem. Eng. 5 (2017) 33–44. https://doi.org/10.4236/msce.2017.54004.
18. Y. Yi, G.S. Was. Stress and temperature dependence of creep in alloy 600 in primary water. Metall. Mater. Trans. A 32, (2001) 2553–2560. https://doi.org/10.1007/s11661-001-0045-6ю
19. D. Karthik, S. Swaroop. Laser shock peening enhanced corrosion properties in a nickel based nconel 600 superalloy. J. Alloys Compd. 694 (2017) 1309–1319. https://doi.org/10.1016/j.jallcom.2016.10.093.
20. N. Makuch, M. Kulka. Microstructural characterization and some mechanical properties of gas-borided Inconel 600-alloy. Appl. Surf. Sci., 314 (2014) 1007–1018. https://doi.org/10.1016/j.apsusc.2014.06.109.
21. ASTM E8-04: Standard Test Methods for Tension Testing of Metallic Materials, ASTM, https://doi.org/10.1520/E0008-04.
22. ASTM E466-21: Standard Practice for Conducting Force Controlled Constant Amplitude Axial

Fatigue Tests of Metallic Materials, ASTM, https://doi.org/10.1520/E0466-21.

23. R.P. Skelton. H.J. Maier, H.J. Christ. The Bauschinger effect, Masing model and the Ramberg– Osgood relation for cyclic deformation in metals. Mater. Sci. Eng. A, 238 (1997) 377–390. https://doi.org/10.1016/S0921-5093(97)00465-6.
24. A. Niesłony, C. Dsoki, H. Kaufmann, P. Krug. New method for evaluation of the Manson–Coffin–Basquin and Ramberg– Osgood equations with respect to compatibility. Int. J. Fatigue 30 (2008) 1967–1977. https://doi.org/10.1016/j.ijfatigue.2008.01.012.
25. Y. Weixing, X. Kaiquan, G. Yi. On the fatigue notch factor, K_f. Int. J. Fatigue 17(4) (1995) 245–251. https://doi.org/10.1016/0142-1123(95)93538-D.
26. N.E. Dowling. Mechanical behavior of materials, engineering methods for deformation, fracture, and fatigue. fourth ed., Pearson, 2013.
27. J. Zhang. C. Zhang, S. Mu, S. Wang, H. Li. Characterization of mechanical properties of in-service nickel-based alloy by continuous indentation. Structures 48 (2023) 1346–1355. https://doi.org/10.1016/j.istruc.2023.01.053.